Journal of Thermal Engineering, Vol. 4, No. 3, pp. 1939-1953, April, 2018
Yildiz Technical University Press, Istanbul, Turkey

INVESTIGATION OF THE EFFECT OF THE PRIMARY NOZZLE THROAT DIAMETER ON THE EVAPORATOR PERFORMANCE OF AN EJECTOR EXPANSION REFRIGERATION CYCLE

C. Seckin[1,*]

ABSTRACT

The present work aims to perform the thermodynamic analysis of an ejector expansion refrigeration cycle (EERC) with a constant-pressure two phase flow ejector and to present the effect of primary nozzle throat diameter on cooling capacity of the EERC. The refrigerant is R134a. In order to achieve these objectives, a computational program is developed using EES software to simulate the system. Mathematical modeling of EERC and applied computational procedure are reported in detail. Operation under critical mode is favorable in ejector operation in terms of high entrainment ratio and enhanced ejector performance. As a result, in this present study, ejector of the refrigeration cycle operates under critical conditions and normal shock occurs at the end of the constant area mixing section. Not an iteration process but Henry and Fauske model is applied to determine the physical properties of the fluid under critical conditions.

Keywords: *Ejector, Ejector Expansion Refrigeration, Constant-Pressure Ejector, Two-Phase Ejector*

INTRODUCTION

In recent years, ejectors have received much attention in stationary and mobile air-conditioning applications due to their ability in throttling loss reduction and increase of system efficiency. The expansion losses by an isenthalpic throttling process are a major irreversibility that contributes to the low energy efficiency of the vapor-compression refrigeration cycles. When an ejector is used to replace the expansion valve in the refrigeration cycle, the expansion work lost during isenthalpic expansion process will be recovered by the ejector to increase the evaporator outlet pressure to a higher pressure before the compressor. The compression work may be saved to increase the COP of the system. While most of the studies are performed for transcritical applications of high pressure fluids, i.e. carbon dioxide, later thermodynamic analyses showed that ejectors offer remarkable efficiency improvement in refrigeration systems working with low pressure refrigerants, as well. At low pressures (in subcritical region) the phase of the substance is saturated mixture while passing through the ejector and "two phase ejector" name is employed to emphasize the existence of two phase together in the ejector. A two-phase ejector performs expansion, mixing and compression of the refrigerant fluxes consecutively. When the high pressure motive fluid moves through the convergent – divergent nozzle (which accelerates the flow velocity from subsonic to supersonic) a low pressure region is created just outside the nozzle (based on Bernoulli's principle). Pressure difference between the secondary flow and low pressure region provides the required suction effect for the secondary flow and the secondary flow gets entrained into the ejector. Then these two flows mix and momentum transfer occurs between the flows (momentum of the motive flow is used to increase the momentum of secondary flow). The mixture is then decelerated through the mixing section and the diffuser increases the pressure of the refrigerant. The result is that pressure of the secondary flow is higher than its initial pressure at the exit of the two-phase flow ejector; i.e. the ejector provides a pressure increase to the lower pressure (secondary) flow. Ejectors allow the expansion process to get closer to isentropic expansion process in comparison to that of conventional vapor compression refrigeration cycle (CVCRC) and reducing the thermodynamic loss of the cycle. As a result, replacing the throttling valve in the CVCRC by an ejector as an expansion device arises as one of the efficient ways to reduce the throttling losses or the expansion irreversibility in the refrigeration cycle. Second, ejector reduces the compressor work by raising the refrigerant pressure to a higher level than evaporator pressure which leads to the improvement of COP of the refrigeration cycle. Hence, it can be stated that the use of two- phase ejector has become a promising modification in refrigeration technology [1-6].

One of the first studies of two-phase ejector use in refrigeration cycle is performed by Gay [7] to

This paper was recommended for publication in revised form by Regional Editor Tolga Taner
[1] Corresponding author. Department of Mechanical Engineering, Engineering Faculty, Marmara University, Istanbul, TURKEY
**E-mail address: candeniz.seckin@marmara.edu.tr, denizseckin1@gmail.com*
Manuscript Received 2 March 2017, Accepted 13 June 2017

recover some of the expansion work that would have otherwise been lost in the classical vapor compression refrigeration cycle (VCRC). Kornhauser [8] proposed a thermodynamic model to analyze the ejector in EERC and found theoretical COP improvements of 21 % (with R12 as the working fluid) over VCRC operating under the same conditions. Elbel and Hrnjak [9] presented an experimental study of EERC with a two-phase ejector and concluded that ejector use in refrigeration systems is efficient notably with high pressure refrigerants (e.g. carbon dioxide) due to the high potential of expansion work recovery. However, lower pressure refrigerants which operate in low pressure refrigeration cycles provides the advantage of better liquid distribution and lower mass flow rate (resulting in lower pressure drop) in the evaporator. Harrell and Kornhauser [10] reported experimental results with an ejector system using R134a and determined COP improvements of 3.9 - 7.6 % over VCRC.

Some of the remarkable two phase flow constant pressure ejector studies in the literature are: an experimental and theoretical study for a constant pressure two-phase flow ejector refrigeration cycle is performed by Disawas and Wongwises [11] and Wongwises and Disawas [12] with R-134a as the working fluid. The effect of operational parameters (such as primary nozzle throat diameter, motive flow mass flow rate, secondary flow mass flow rate, average evaporator pressure, cooling capacity) on system COP is investigated. Wang and Yu [13] presented an experimental investigation on two-phase driven ejector performance characteristics in an EERC using R600a as the refrigerant. Tashtoush et al. [14] selected ejector refrigeration cycle with refrigerant R134a as the basic cycle and investigated the performance of other refrigerants only at critical mode.

In practice, there are two choking phenomena which strictly effect the ejector performance 1) motive flow passing through the primary nozzle and 2) choking of the secondary flow [15,16]. The second choking results from the velocity increase of the secondary flow from a stagnant state to a supersonic flow in the constant-area mixing section. The ejector performance can be divided into three operational modes, according to the back pressure of the ejector: the critical, subcritical and back flow modes. Relation of these modes with back pressure and the variation of entrainment ratio (w) is depicted in Figure 1 (based on [17]). The entrainment ratio remains constant with increasing back pressure until the back pressure reaches the critical point (Pc*), after which further increase in the back pressure results in a sharp decrease in entrainment ratio. When the ejector is operated at the critical mode, the cooling capacity and COP remain constant. Further increase in the backpressure above the critical pressure moves the normal shock wave into the mixing zone and prevents the secondary flow from chocking and reaching sonic velocity. The highest performance of an ejector is reached at the critical mode due to high entrainment ratio and constant cooling capacity. Detailed explanation is available in [2,14,17,18].

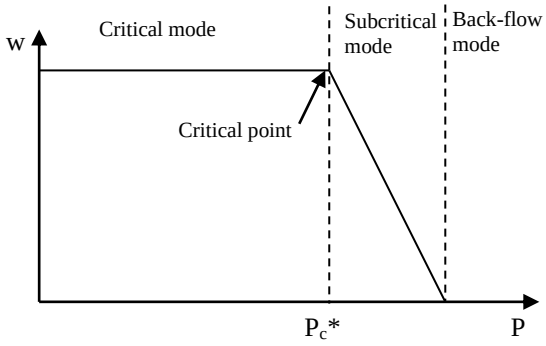

Figure 1. Operational modes of ejector

In this present study, variation of primary nozzle throat diameter with cooling capacity is analyzed for a constant pressure type ejector used in an EERC. The ejector operates at critical mode, i.e. the motive and secondary flows are both chocked and the entrainment ratio is constant [19]. The considered ejector cooling cycle is simulated with EES Software. In order to eliminate the analytical error induced by the ideal gas assumption when the ejector issued with refrigerants, the thermodynamics properties of real gases were used [20-22] to apply mass, momentum, and energy conservation principles. Normal shock occurs at the end of the constant area mixing chamber [19,23,24]. Systematic of ejector modeling is similar to that of [19] but in this present study, 1) design of the analyzed ejector refrigeration cycle (EERC) is different and 2) thermodynamic

properties of the fluid at critical conditions are determined by Henry and Fauske method (i.e. an iterative computational procedure is not applied as applied in [19]). Details and use of Henry and Fauske method in computation are extensively discussed in further sections of this study.

EERC AND EJECTOR DESIGN

Schematic of ejector expansion refrigeration cycle (EERC) and P-h diagrams of the considered EERC are presented in Figure 2-a,b. Main components of EERC are: a compressor, a condenser, an expansion valve, an evaporator, a separator and a two-phase flow ejector as the key component of the cycle. The refrigerant R134a exits the ejector in saturated mixture phase (state point 6, Figure 2) and enters into the separator. In the separator, the refrigerant is divided into two streams: saturated vapor and saturated liquid parts. Saturated vapor part is transferred to the compressor where the pressure and temperature of the fluid are raised to those of the condenser. The superheated vapor phase refrigerant at the exit of the compressor is delivered to the condenser. Then, superheated vapor refrigerant condenses in the condenser and discharges heat to the surrounding as a result of the condensation process. At the exit of the condenser, the phase of the refrigerant is saturated liquid and enters the ejector at condenser pressure and temperature (state point 1, Figure 2). The other part (saturated liquid part in the separator, state point 7) circulates the lower loop (refrigeration loop). The refrigerant enters into the expansion valve after leaving the separator and the pressure and temperature of the saturated liquid are dropped to those of the evaporator (state point 8, Figure 2). In the evaporator, refrigeration takes place, i.e., heat is extracted from the conditioned space and is transferred to the refrigerant. The refrigerant vaporizes while passing through the evaporator. After the evaporator (state point 2, Figure 2) the refrigerant is in saturated vapor phase and is at evaporator pressure/temperature.

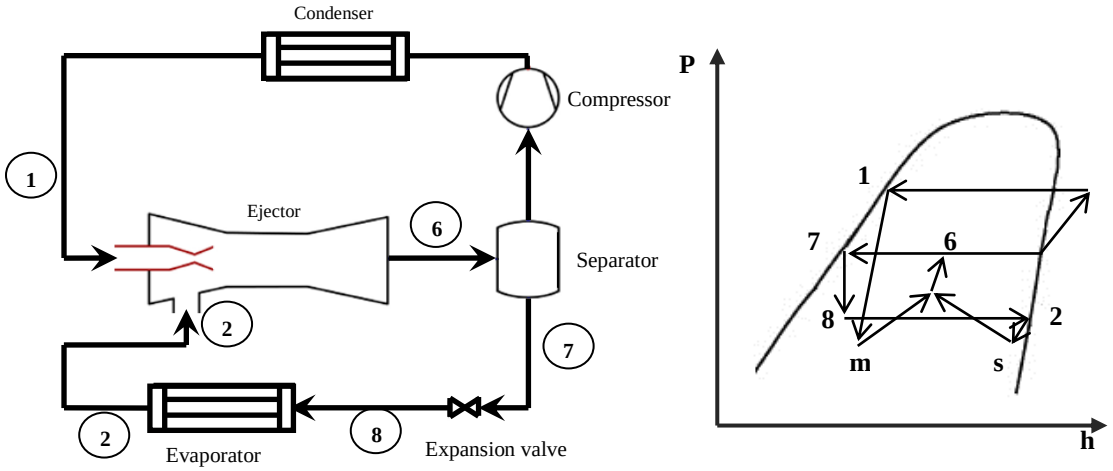

Figure 2. a) Schematic overview of EERC b) P-h diagram of EERC

The ejector design can be classified into two categories depending on the exit location of the nozzle: "constant area ejector" and "constant pressure ejector". When the exit of the nozzle is located within the constant area mixing section, mixing takes place in the mixing section and the ejector is named as "constant-area ejector". The ejector is named "constant pressure ejector" when the exit of the nozzle is located within the "suction chamber" which is in front of the constant-area mixing section. In constant pressure ejector, it was assumed that the mixing takes place in the suction chamber and the pressure is constant in the suction chamber [17,25]. In this study, analysis of a "constant-pressure ejector" in EERC is performed and results are presented in details.

Schematic representation of the considered constant pressure ejector is presented in Figure 3. It consists of a convergent–divergent nozzle (primary nozzle), a converging nozzle (secondary nozzle), mixing chamber and a diffuser. Refrigerant which comes from the condenser enters the convergent–divergent nozzle at state 1 (named motive stream hereinafter) and is chocked at its throat before expanding to a very low static pressure at nozzle exit. In the nozzle, the refrigerant is accelerated to supersonic velocity. The pressure difference between the primary nozzle exit and the evaporator provides the required suction for the refrigerant at state 2 (named secondary stream hereinafter) to enter into the ejector. As the "constant pressure ejector" name implies, exit pressure of the motive stream and the secondary stream is the same and pressure is constant through the suction

chamber. The motive and the secondary streams flow separately without mixing in the suction chamber, and then both of the fluids mix in the mixing chamber. Mixing process ends at cross-section 3 in Figure 3. A shock wave occurs at the end of the constant area mixing section which causes reduction in mixture velocity from supersonic to subsonic and increase in the pressure (cross-section 4, Figure 3). At the end of the mixing chamber (cross-section 5, Figure 3), the refrigerant enters into the diffuser in which the velocity of the mixed fluid is stepped down and the pressure is lifted to the condenser pressure (cross-section 6, Figure 3) [1,25].

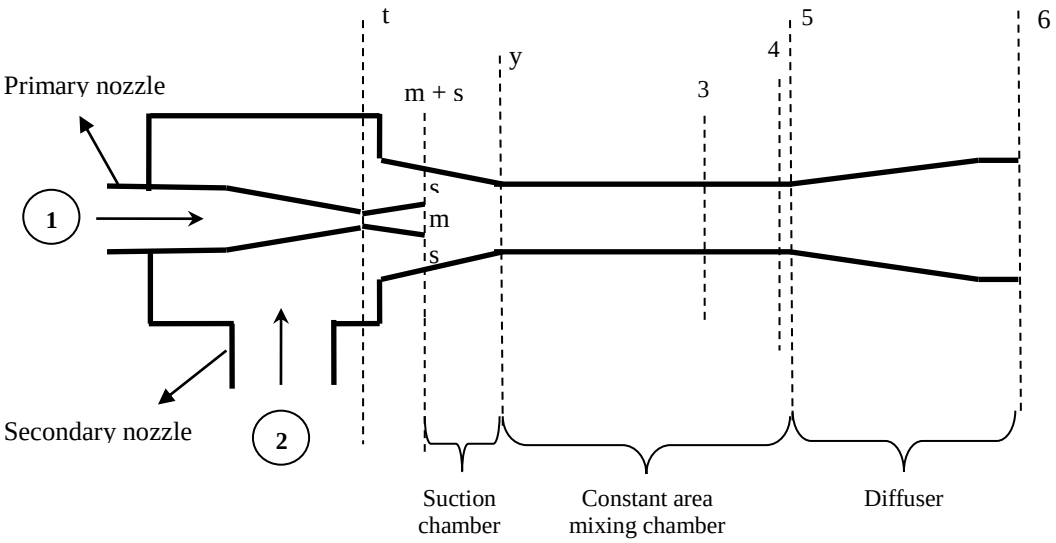

Figure 3. Schematic diagram of the constant pressure ejector

MATHEMATICAL MODELING AND COMPUTATIONAL PROCEDURE

The ejector is the key component of EERS since it recovers the expansion process losses and increases the compressor inlet pressure. The mathematical representation of the flow inside the ejector and the EERC is very complex. Besides the conservation equations of mass, energy and momentum, state equations, phase change principle, isentropic relations as well as some appropriate assumptions need to be used to assist in the description of the flow and mixing in the two-phase ejector [26]. Below, governing equations which are developed to determine the working characteristics of the ejector and the other components of EERC are presented.

In the analysis, conservation of mass, energy and momentum equations are successively applied to each part of the ejector and the other components of the EERC (Figures 2,3). Following assumptions are applied [23,27,28]:

1. One-dimensional, steady state and adiabatic flow through the ejector.
2. Motive and secondary fluids are supplied at zero velocities (i.e. stagnation conditions) at state points (1) and (2). Also, velocity of compressed mixture at the exit of diffuser (state point 6 in Figure 3) is zero (stagnation condition).
3. Pressure is constant in the suction chamber.
4. Friction losses are defined in terms of isentropic efficiencies in the nozzles and diffuser.
5. The design pressure at the primary nozzle exit is uniform and the secondary stream velocity reaches the speed of sound at this level.
6. Critical-mode operation, i.e. the motive and secondary flows are both chocked and the entrainment is constant.
7. Normal shock occurs at the end of the constant area mixing chamber.
8. The heat transfer between the fluid and ejector wall is neglected.
9. The gravitational force effect on the flow is neglected.

Mathematical formulas for thermodynamic modeling of the refrigeration system are reported below for each part of the ejector and components of the cycle.

Secondary nozzle

In a real ejector, the secondary nozzle is typically replaced by a suction chamber. However, to simplify the analysis, the expansion process from the state point 2 to the cross-section s (see Figure 3) is treated in the same way as the expansion process of a converging nozzle.

By definition of constant pressure ejector, it is assumed that the motive stream and the secondary stream mixed at critical pressure of the secondary stream (critical conditions, $P_m = P_s$ and Ma=1 at cross-sections) [19,27]. Consequently, an iterative process is applied to determine the critical pressure of the secondary fluid by Henry and Fauske method and details are available in this section. In summary, the exit pressure and velocity of the secondary stream is determined by the given inlet flow conditions and its isentropic efficiency. Using a specified mass flow rate, exit area is determined as well.

Using the definition of secondary nozzle's isentropic efficiency (h_s), the specific enthalpy of the secondary fluid at the nozzle exit (h_s) is given by the following expression:

$$h_s = h_2 (1-\eta_s) + \eta_s \, h_{s,is} \tag{1}$$

$$h_{s,is} = f(P_s, s_2) \tag{2}$$

where $h_{s,is}$ is the specific enthalpy of the secondary stream at the end of the isentropic expansion process in the secondary nozzle, h_2 is the specific enthalpy of the secondary stream at the nozzle inlet, P_s is the secondary stream pressure at the secondary nozzle exit, s_2 is the specific entropy of the secondary stream at the nozzle inlet.

Based on conservation of energy principle, velocity of the secondary stream at the secondary nozzle exit (V_s) is determined by the following:

$$V_s = \sqrt{2 (h_2 - h_s)} \tag{3}$$

Based on the conservation of mass equation, below equations must be satisfied at the exit of the secondary nozzle:

$$m_2 = \left(\frac{w}{1+w} \right) m_{tot} = \frac{V_s \, A_s}{v_s} \tag{4}$$

$$v_s = f(P_s, h_s) \tag{5}$$

$$x_s = f(P_s, h_s) \tag{6}$$

where w is the entrainment ratio which is the ratio of the secondary stream mass flow rate (m_2) to the motive stream mass flow rate (m_1), m_{tot} is the total mass flow rate of the refrigerant (m_1+m_2), A_s and v_s are the cross-sectional area and the specific volume at the secondary nozzle exit, respectively. x_s is the quality of secondary stream at nozzle exit.

Primary nozzle

Using the definition of primary nozzle's isentropic efficiency (h_p), the specific enthalpy of the motive fluid at the nozzle exit (h_m) is given by the following expressions:

$$h_m = h_1 (1-\eta_p) + \eta_p \, h_{m,is} \tag{7}$$

$$h_{m,is} = f(P_m, s_1) \tag{8}$$

where $h_{m,is}$ is the specific enthalpy of the motive stream at the end of the isentropic expansion process in the primary nozzle, h_1 is the specific enthalpy of the motive stream at the nozzle inlet, P_m is the motive stream pressure at the primary nozzle exit, s_1 is the specific entropy of the motive stream at the nozzle inlet.

Based on conservation of energy principle, velocity of the motive stream at the primary nozzle exit (V_m) is determined by the following:

$$V_m = \sqrt{2\,(h_1 - h_m} \tag{9}$$

Based on the conservation of mass equation, below equations must be satisfied at the exit of the primary nozzle:

$$m_1 = \left(\frac{1}{1+w}\right) m_{tot} = \frac{V_m\ A_m}{v_m} \tag{10}$$

$$v_m = f\,(P_m, h_m) \tag{11}$$

where A_m and v_m are the cross-sectional area and the specific volume at the primary nozzle exit, respectively.

Suction chamber and constant area mixing chamber

This part starts from the exits of the nozzles (cross-section m+s in Figure 3) to the cross-section 5 in Figure 3. To simplify the model of this part, the following assumptions are made:

- At the inlet plane (m), the motive stream has a velocity of V_m, a pressure of P_m, and occupies the area A_m.
- At the inlet plane (s), the secondary stream has a velocity of V_s, a pressure of P_s (= P_m), and occupies the area A_s.
- At the cross -section 3, the flow becomes uniform and has the velocity of V_3 and pressure of P_3.
- The motive stream pressure and secondary stream pressure keep unchanged from the nozzle exits until the inlet of the constant area mixing section (between (m+s) – (y)). There is no mixing between the motive stream and secondary stream before the inlet of the constant area mixing chamber.

Motive and secondary streams preserve their identity over a short distance following the exit from their respective nozzles, before mixing takes place. This distance corresponds to distance between cross-section (m+s) and cross-section (y) in Figure 3. [19,27]. Mixing is assumed to occur at constant pressure over a short distance in the mixing chamber (between cross-sections y and 3 in Figure 3), in the ejector cross-section the pressure is uniform and corresponds to the critical pressure of the secondary stream [27]. Hence,

$$A_{m+s} = A_s + A_m \cong A_4 = A_5 \tag{12}$$

Since the distance between (m+s) and (y) is very short, friction losses are not accounted for in this region. Based on mass, momentum and energy conservation equations, the enthalpy and velocity of the mixed fluid at the end of the mixing chamber can be calculated using the following equations:

$$m_{tot} = m_1 + m_2 = (1+w)\ m_1 = \left(1+\frac{1}{w}\right) m_2 \tag{13}$$

Conservation of mass equation:

$$m_{tot} = \frac{V_4\ A_4}{v_4} \tag{14}$$

where V_4 and v_4 are velocity and specific volume of the refrigerant at cross-section 4 in Figure 3, respectively.

Conservation of momentum equation:

$$P_4\ A_4 + m_{tot}\ V_4 = \varphi_m\ (P_m\ A_m + m_1\ V_m + P_s\ A_s + m_2\ V_s)$$
$$= P_4\ A_4 + \frac{A_4\ V_4^2}{v_4} = \varphi_m \left(P_m\ A_m + \frac{A_m\ V_m^2}{v_m} + P_s\ A_s + \frac{A_s\ V_s^2}{v_s} \right) \quad (15)$$

In above equations, P_4 is the pressure of the mixed flow at the end of the constant area mixing section (before shock), φ_m is the coefficient accounting for the frictional loss [17].

Under the assumption of P_4 is known, inserting A_4 and m_{tot} into the Eq. (15), V_4 can be determined. After determining V_4, v_4 is also obtainable from Eq. (14).

Conservation of energy equation:

$$m_t \left[h_4 + \frac{V_4^2}{2} \right] = m_1 \left[h_m + \frac{V_m^2}{2} \right] + m_2 \left[h_s + \frac{V_s^2}{2} \right] \quad (16)$$

Inserting V_4 into Eq. (16), h_4 (specific entropy at cross-section 4) can be determined. Then,

$$h_4 = f(P_4, v_4) \quad (17)$$

$$x_4 = f(P_4, h_4) \quad (18)$$

Eq. (17) must be satisfied.

The normal shock is assumed to occur at the end of mixing chamber, i.e., Ma=1 at the cross-section 4. To achieve this condition, flow must be critical flow at the end of the constant area mixing section. If the phase of the substance is saturated mixture, then Henry and Fauske method is applied to determine the fluid properties before shock (presented in this section). If the phase is superheated mixture, below procedure is applied:

$$Ma=1 = \frac{V_4}{C_4} \quad (19)$$

$$C_4 = f(P_4, h_4) \quad (20)$$

where C_4 is the speed of sound at cross-section 4 (before shock). Pressure of the mixed fluid at the end of the mixed section just before shock wave (P_4) is iterated until Mach number at the mixed section reaches unity.

Because the distance between cross-section 4 and 5 in which this normal shock takes place is very narrow, it may be considered that the area change across the shock wave is negligible and the flow is adiabatic [29]. Conservation of mass, momentum, energy equations as well as entropy balance before and after the normal shock are applied as presented below [19,30]:

Conservation of momentum equation:

$$P_4\ A_4 + m_{tot}\ V_4 = P_5\ A_5 + m_{tot}\ V_5 \Rightarrow V_5 = \frac{(P_4 - P_5)\ A_5}{m_{tot}} + V_4 \quad (21)$$

Conservation of mass equation:

$$m_4 = m_5 \Rightarrow \frac{A_4\ V_4}{v_4} = \frac{A_5\ V_5}{v_5} \Rightarrow v_5 = \frac{V_5\ v_4}{V_4} \quad (22)$$

Conservation of energy equation:

$$h_4 + \frac{V_4^2}{2} = h_5 + \frac{V_5^2}{2} \tag{23}$$

$$s_5 = f(P_5, v_5) \tag{24}$$

$$s_5 > s_4 \tag{25}$$

where A_5, P_5, V_5, v_5, h_5 and s_5 are area, pressure, velocity, specific volume, specific enthalpy and specific entropy at the cross-section 5, respectively.

Diffuser

Specific enthalpy at the diffuser exit (h_6) can be obtained by applying conservation of energy:

$$m_{tot}\, h_6 = m_1\, h_1 + m_2\, h_2 \tag{26}$$

In addition to this, h_6 could be determined by Eq. (27) where η_d is the diffuser isentropic efficiency, $h_{6,is}$ is the specific enthalpy at the end of the isentropic process in the diffuser, P_6 is the pressure at the exit of the diffuser and s_5 is the specific entropy at the diffuser inlet (after shock).

$$\eta_d = \frac{h_{6,is} - h_5}{h_6 - h_5} \tag{27}$$

$$h_{6,is} = f(P_6, s_5) \tag{28}$$

The diffuser outlet quality (x_6) is obtained from thermodynamic property relation:

$$x_6 = f(P_6, h_6) \tag{29}$$

In order to realize the cycle, the relation between the entrainment ratio (w) and the ejector outlet quality (x_6) presented in Eq. (30) must be satisfied.

$$x_6\,(1+w) = 1 \tag{30}$$

Evaporator

As reported above, the separator has 100% efficiency and refrigerant exits from the separator at saturated conditions. Then:

$$h_7 = f(P_6, x = 0) \tag{31}$$

Performing energy equation between inlet and outlet of the expansion valve gives the below equation:

$$h_7 = h_8 \tag{32}$$

Then, energy transfer rate to the fluid passing through the evaporator (cooling capacity of the cycle, Q_{evap}) is derived by the below equation:

$$Q_{evap} = m_2 (h_2 - h_8) \tag{33}$$

Determination of critical flow properties

The main parts of the considered two-phase flow ejector are: the primary nozzle, the secondary nozzle, the constant area mixing section and the diffuser, as seen in Figure 3. Above presented thermo-fluid based mathematical model aims to determine diameters of these main parts of the ejector.

As stated in earlier sections, in this present study, a constant pressure ejector is analyzed under the critical operation mode conditions, i.e., the motive and secondary flows are both chocked and the entrainment is constant. In addition to this, normal shock takes place at the end of the constant area mixing chamber, i.e. flow is critical at the end of the chamber (cross-section 4 in Figure 3). Considered ejector is a two phase flow ejector, hence, at the cross-section (t) for the primary nozzle and at the cross-section (s) for the secondary nozzle, the flows are two-phase critical flow. In this study, diameters and flow properties at these critical cross-sections are determined according to the empirically determined flow model provided by Henry and Fauske [31]. It is noteworthy to elucidate that Henry and Fauske [31] reported experimental results with R744 to validate their model which is the prevailing reason of using their method in this study. In the literature, Henry- Fauske model is used in several experimental and theoretical works [11,12,32,33].

It is stated in earlier section that, after mixing of motive and secondary fluxes takes place in the constant area mixing chamber (cross-section 3 in Figure 3), mixed flow becomes supersonic and normal shock occurs at the end of the constant area mixing section. It is also possible that, the flux remains as a two-phase flow (i.e., does not become supersonic) in the mixing chamber depending on operational conditions. For this case, shock does not ocur in the mixing chamber but critical flow conditions must also be obtained before the difuser (cross-section 5 in Figure 3) to have maximum possible pressure of the flux at the end of the constant area mixing chamber.

Using Henry and Fauske method, the critical mass flux of the mixture flow can be calculated by simultaneous solving of Eq. (34) and (35) [31].

$$G_c^2 = \left[\frac{x_0 v_g}{n P} + (v_g - v_{l0}) \left\{ \frac{(1-x_0) N}{s_g - s_l} \frac{ds_l}{dP} - \frac{x_0 c_{gp} (1/n - 1/\gamma)}{P (s_{g0} - s_{l0})} \right\} \right]_t^{-1} \tag{34}$$

$$(1-x_0) v_{l0} (P_0 - P_t) + \frac{x_0 \gamma}{\gamma - 1} (P_0 v_{g0} - P_t v_{gt}) = \frac{\left[(1-x_0) v_{l0} + x_0 v_{gt} \right]^2}{2} G_c^2 \tag{35}$$

where N is the partial phase change at the throat and is determined experimentally as presented in Eq. (36). G_c is the critical mass flux (mass flow rate per unit cross-sectional area at the throat) as seen in Eq. (37).

$$N = \begin{cases} x_t/0.14 & 0 < x_t < 0.14 \\ 1 & x_t > 0.14 \end{cases} \tag{36}$$

$$G_c = \frac{m}{A} \tag{37}$$

n [31] and γ [34] are computed based on the equations:

$$n = \frac{(1-x) \left[(c_l / c_g)_p \right] + 1}{(1-x) \left[(c_l / c_g)_p \right] + 1/\gamma} \tag{38}$$

$$\gamma = \frac{c_P}{c_V} \tag{39}$$

where subscript 0 refers to input condition of the expanding fluid. Subscripts g and l signify vapor and liquid phase of the the refrigerant. Subscript t represents the property of the fluid at throat (fluid under critical conditions).

Secondary nozzle exit

Above presented Henry and Fauske method equations (Eq. (34)-(39)) are applied to determine the secondary stream properties at the secondary nozzle exit. Formulas are presented below:

$$G_{c,s} = \frac{m_2}{A_s} \tag{40}$$

$$x_2 = x_0 = 1 \tag{41}$$

Inserting Eq. (41) into Eq. (38) gives:

$$n = \gamma \tag{42}$$

In Henry and Fauske method, expansion process is assumed to be isentropic. Based on Eq. (41) and Eq. (42), Eq. (34) becomes:

$$G_{c,s}^2 = \left[\frac{v_g}{n P}\right]_t^{-1} \tag{43}$$

Inserting Eq. (43) into Eq. (35) and applying isentropic process equation (based on [31]), Eq. (35) reduces to:

$$\left[v_{gt}\right]_s^{\gamma-1} = \left[v_{go}\right]_s^{\gamma-1} \left[(\gamma-1)\left(\frac{1}{2} + \frac{1}{\gamma-1}\right)\right] \tag{44}$$

where $[v_{go}]_s$ is the specific volume of the saturated vapor at the secondary nozzle inlet pressure and temperature which is equal to v_2 in Figure 2. $[v_{gt}]_s$ is the specific volume of the saturated vapor at the throat of the secondary nozzle which is the exit of the nozzle.

$$\left\lfloor v_{go} \right\rfloor_s = v_2 \tag{45}$$

After determination of $[v_{gt}]_s$, throat pressure (P_s) is determined based on Eq. (46).

$$P_s = f\left(v = \left\lfloor v_{gt} \right\rfloor_s, x = 1\right) \tag{46}$$

An alternative way of determining A_s is inserting P_s into Eq. (43) to determine $G_{c,s}$ and substituting $G_{c,s}$ into Eq. (40). The deviation of A_s which is determined by applying the computational procedure between Eq. (40-46) and by this alternative way is checked. It is seen that deviation is strongly negligible.

Primary nozzle throat

Above presented Henry and Fauske method equations (Eq. (34-39)) are applied to determine the motive stream properties at the primary nozzle throat. Formulas are presented below:

$$x_1 = x_0 = 0 \tag{47}$$

$$P_0 = P_1 \tag{48}$$

$$v_{l0} = v_1 \tag{49}$$

Eq. (47-49) is substituted into Eq. (35) to obtain Eq. (50). Gc,m can be determined from Eq. (50).

$$\left[\frac{P_{t,m}}{P_0}\right] = 1 - \frac{v_{l0}\ G_{c,m}^2}{2\ P_0} \tag{50}$$

Cross-sectional area of primary nozzle throat can be determined as:

$$G_{c,m} = \frac{m_1}{A_{t,m}} \quad \Rightarrow A_{t,m} = \frac{m_1}{G_{c,m}} \tag{51}$$

Using the definition of primary nozzle's isentropic efficiency (η_p), the specific enthalpy of the motive fluid at the nozzle throat ($h_{t,m}$) is given by the following expression:

$$h_{t,m} = h_1\,(1-\eta_p) + \eta_p\ h_{t,m,is} \tag{52}$$

$$h_{t,m,is} = f\,(P_{t,m}, s_1) \tag{53}$$

where η_p is the primary nozzle isentropic efficiency, $h_{t,m,is}$ is the specific enthalpy of the motive stream at the throat of the primary nozzle by an isentropic expansion process, h_1 is the specific enthalpy of the motive stream at the nozzle inlet, $P_{t,m}$ is the motive stream pressure at the primary nozzle throat, s_1 is the specific entropy of the motive stream at the nozzle inlet.

Based on the conservation of energy principle, velocity of the motive stream at the primary nozzle throat ($V_{t,m}$) is determined by the following:

$$V_{t,m} = \sqrt{2\,(h_1 - h_{t,m})} \tag{54}$$

Based on the conservation of mass equation, below equation must be satisfied at the throat of the primary nozzle:

$$m_1 = \left(\frac{1}{1+w}\right) m_t = \frac{V_{t,m}\ A_{t,m}}{v_{t,m}} \Rightarrow v_{t,m} = \frac{V_{t,m}\ A_{t,m}}{m_1} \tag{55}$$

$$P_{t,m} = f\,(v_{t,m}, h_{t,m}) \tag{56}$$

where $v_{t,m}$ is the specific volume of the motive stream at the throat of the nozzle, $A_{t,m}$ and $v_{t,m}$ are the cross-sectional area and the specific volume at the primary nozzle throat, respectively.

Cross-section 4

If the phase of the fluid is saturated mixture at the end of the constant are mixing section, Eq. (35) is used by inserting below equations:

$$G_{c,4} = \frac{m_t}{A_4} \tag{57}$$

$$v_{lo} = f\ (P = P_s, x = 0) \tag{58}$$

$$v_{go} = f\ (P = P_s, x = 1) \tag{59}$$

$$v_{gt} = f\ (P = P_4, x = 1) \tag{60}$$

RESULTS AND DISCUSSION

Variation of primary nozzle throat diameter with respect to cooling performance of the considered ejector expansion refrigeration cycle (EERC) is analysed using developed formulas in Section 3 which pertain to ejector and EERC design. Results are generated to determine the primary nozzle throat dimension using R134a as the refrigerant, primary and secondary nozzle isentropic efficiency of 90%, diffuser efficiency of 85%. Analyzed constant pressure ejector operates under critical flow conditions, i.e,. the motive and secondary flows are both chocked hence the entrainment ratio (w) is constant. Saturated exit conditions are provided for evaporator and condenser. The ejector is designed in such a manner so that normal shock occurs at the end of the constant area mixing chamber. The analysis is performed over a wide range of cooling capacity and design dimensions of the ejector. Developed simulation program determines the ejector dimensions at highest possible performance characteristics due to critical flow conditions (during critical mode operation, the motive and secondary flows are both choked, and the entrainment ratio reaches a maximum value that remains constant with lower values of back pressure. It must be also stated that over the range of investigated condenser and evaporator temperatures (and pressures), mixed flow is a supersonic flow at the end of the constant area mixing chamber (cross-section 4 in Figure 3) and this is where normal shock occurs.

Graphical results of variation in primary nozzle throat diameter versus cooling capacity is presented in Figure 4 for condenser temperature of 50, 60 and 70 °C and evaporator temperature of 0°C. Numerical results show that entrainment ratio (w) gets lower and dimension of the primary nozzle throat ($A_{t,m}$) gets higher with increasing T_{cond} (T_1). It is also interesting that for constant T_{cond} and $T_{evap,}$ w is constant for increasing Q_{evap}. Explaining the relation of w with other system parameters is out of the scope of this study and would also result in a crowding of different concepts in a single paper. However, system parameters including w are reported in Table 1 since w has a considerable effect on increasing primary nozzle throat diameter with increasing T_{cond}.

Results can be explained in such a way that, condenser pressure P_1 is the P_0 term in Eq. (50). Corresponding P_1 values are also getting larger with increasing T_{cond} (T_1). The effect of increasing P_0 is balanced with increasing $G_{c,m}$ and $P_{t,m}$ values in Eq. (50). As a result of decreasing w, m_1 values gets higher based on Eq. (10) as T_{cond} increases. However, since the increasing rate of m_1 is higher relative to that of $G_{c,m}$, $A_{t,m}$ values gets higher with increasing T_{cond} based on Eq. (51). Results are presented in Table 1.

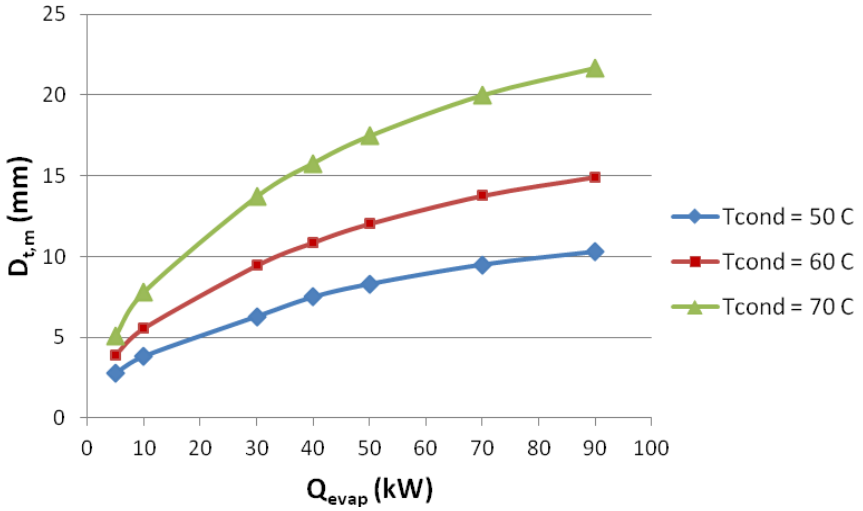

Figure 4. Variation of ejector primary nozzle diameter ($D_{t,m}$) with cooling capacity (Q_{evap})

Table 1. Variation of P_1, m_1, w, $P_{t,m}$, $G_{c,m}$, $A_{t,m}$ and $D_{t,m}$ with T_{cond} (Q_{evap}= 10 kW and 50 kW)

Q_{evap} = 10 kW							
T_{cond} (°C)	**P_1 (kPa)**	**m_1 (kg/s)**	**w**	**$P_{t,m}$ (kPa)**	**$G_{c,m}$ (kg/m^{2}s)**	**$A_{t,m}$ (mm^2)**	**$D_{t,m}$ (mm)**
50	1319	0.144	0.74	1249.11	12412.48	11.58	3.84
60	1683	0.151	0.66	1664.84	6183.75	24.35	5.57
70	2118	0.158	0.58	2112.49	3313.02	47.76	7.80
Q_{evap} = 50 kW							
50	1319	0.144	0.74	1315.78	2656.84	54.08	8.30
60	1683	0.151	0.66	1682.17	1323.46	113.79	12.04
70	2118	0.158	0.58	2117.78	661.95	239.03	17.45

Consequently, throat diameter does not have a direct effect on EERC cooling performance since cooling performance of the cycle is directly prevailed by w and T_{evap}. For constant T_{evap}, w is widely dominated by suction pressure (pressure at the nozzle exit, P_s=P_m) and it is a direct function of T_{evap}. It is inferred from the result of the analysis that throat diameter is not a determining factor on EERC cycle cooling performance and the variation of primary nozzle throat diameter has an exponential relation with cooling performance (Q_{evap}).

CONCLUDING REMARKS

In the present work, a computer program for ejector design and simulation of a ejector expansion refrigeration system (EERS) working with R134a is developed. For design purposes, relation between the main ejector dimensions and the operating parameters are very useful and beneficial. In general, the system cooling capacity has the most significant impact on the ejector design. The simulation aimed at presenting the variation of primary nozzle throat diameter on the cooling performance characteristics of the EERS. The analysis is performed for condenser temperature of 50, 60 and 70 °C and evaporator temperature of 0°C. It is concluded that, nozzle throat dimeter is directly affected by condenser temperature and entrainment ratio. Based on the reported results in Figure 4 and Table 1, the following conclusions can be drawn: there is an exponential mathematical relation between primary nozzle throat diameter and cooling performance of the EERC. Over the analyzed temperature and pressure ranges of evaporator and condenser, mixed flow is a supersonic flow at the end of the constant area mixing section and this is where normal shock takes place. As the condenser temperature increases, primary nozzle diameter also increases.

It must be stated that shock phenomenon is a critical part of ejector operation. It means, an accurate and realistic two – phase ejector model must be able to provide realistic predications for location, shape, and strength of shockwaves. As explained in the earlier sections, physical properties of the shock waves are mainly determined by the Mach number of the fluid flow passing throughout the ejector. However, for two-phase ejector flows (like considered flow in this study), fluid flow regime strongly determines the speed of sound and the regime of the flow through a two-phase ejector is generally not well predicted. Hence, determination of Mach number and accurate prediction of properties of occurred shock wave arise as a difficulty for modeling of two-phase flow ejector. In other words, more accurate knowledge of the flow pattern in above mentioned ejector parts, turbulence modeling, shockwave shape and strength are needed in order to improve the accuracy of ejector models in ejector modeling studies [35,36]. As a result, any further attempts for shock modeling of two-phase flow or prediction of flow regime are very precious to provide accuracy to CFD modeling studies of ejector involving systems, like this present study. Another important point is that the accuracy of the presented results is limited by the fundamental assumptions applied in this study. These assumptions must be regarded as solutions to fulfill the aimed analysis of considered ejector refrigeration system. Since experimental investigation of analyzed system is not yet performed by the author, a sensitivity analysis for each of performed assumptions ought to be carried out. This though exceeds the limits and the goals of the study since the object of the study is presenting the essential details of applied procedure for modeling of ejector expansion refrigeration cycle.

NOMECLATURE

A Cross-sectional area (m^2)
COP Coefficient of performance
h Specific enthalpy (kJ/kg)
Ma Mach number

P	Pressure (kPa)
s	Specific entropy (kJ/kg K)
T	Temperature (°C)
V	Velocity (m/s)
v	Specific volume (m^3/kg)
w	Entrainment ratio
x	Quality
Q	Heat transfer rate (kW)
W	Power (kW)
η	Isentropic efficiency
1,2,3…	Number of points in Figure 2

Subscripts

cond	Condenser
evap	Evaporator
is	Isentropic
m	Primary nozzle
s	Secondary nozzle
t	Throat
tot	Total

REFERENCES

[1] Sarkar, J. (2010). Geometric parameter optimization of ejector-expansion refrigeration cycle with natural refrigerants. International Journal of Energy Research, 34(1), 84-94.

[2] Lawrence, N., Elbel, S. (2012). Experimental and analytical investigation of automotive ejector air conditioning cycles using low-pressure refrigerants. International Proceedings of International Air Conditioning and Refrigeration Conference, 2118-2122.

[3] Gurulingam, S., Kalaisselvane, A., Alagumurthy, N. (2012). Performance improvement of forced draught jet ejector using constant rate momentum change method. International Journal of Engineering and Advanced Technology (IJEAT),2, 149-153.

[4] Dixit, M., Arora, A., Kaushik, S. C. (2016). Energy and exergy analysis of a waste heat driven cycle for triple effect refrigeration. Journal of Thermal Engineering, 2, 954-961.

[5] Kutlu, C., Unal, S., Erdinc, M. T. (2016). Thermodynamic analysis of bi-evaporator ejector refrigeration cycle using r744 as natural refrigerant. Journal of Thermal Engineering, 2, 735-740.

[6] Sarevski, M. N., & Sarevski, V. N. (2016). Characteristics of R718 refrigeration/heat pump systems with two-phase ejectors. International Journal of Refrigeration, 70, 13-32.

[7] Gay, N. H. Refrigerating System. US Patent 1,836,318, 1931.

[8] Kornhauser, A. A. (1990). The use of an ejector as a refrigerant expander. In Proceedings of the 1990 USNCR/IIRPurdue Refrigeration Conference, 10-19.

[9] Elbel, S. W., Hrnjak, P. S. (2008). Experimental validation of a prototype ejector designed to reduce throttling losses encountered in transcritical R744 system operation. International Journal of Refrigeration, 31, 411-422.

[10] Harrell, G. S., Kornhauser, A.A. (1995). Performance tests of a two-phase ejector. In Proceedings of the 30th Intersociety Energy Conversion Engineering Conference, 49–53.

[11] Disawas, S., & Wongwises, S. (2004). Experimental investigation on the performance of the refrigeration cycle using a two-phase ejector as an expansion device. International Journal of Refrigeration, 27(6), 587-594.

[12] Wongwises, S., & Disawas, S. (2005). Performance of the two-phase ejector expansion refrigeration cycle. International journal of heat and mass transfer, 48(19-20), 4282-4286.

[13]Wang, X., & Yu, J. (2016). Experimental investigation on two-phase driven ejector performance in a novel ejector enhanced refrigeration system. Energy Conversion and Management, 111, 391-400.

[14] Tashtoush, B., Alshare, A., Al-Rifai, S. (2015). Performance study of ejector cooling cycle at critical mode under superheated primary flow. Energy Convers. Manage., 94, 300–310.

[15] Munday, J. T., & Bagster, D. F. (1977). A new ejector theory applied to steam jet refrigeration. Industrial & Engineering Chemistry Process Design and Development, 16(4), 442-449.

[16] Huang, B. J., Jiang, C. B., & Hu, F. L. (1985). Ejector performance characteristics and design analysis of jet refrigeration system. Journal of engineering for gas turbines and power, 107(3), 792-802.

[17]Huang, B. J., Chang, J. M., Wang, C. P., & Petrenko, V. A. (1999). A 1-D analysis of ejector performance. International journal of refrigeration, 22(5), 354-364.

[18] Seckin, C. (2017). Parametric analysis and comparison of ejector expansion refrigeration cycles with constant area and constant pressure ejectors. Journal of Energy Resources Technology, 139, 042005-1 - 042005-10.

[19] Khalil, A., Fatouh, M., & Elgendy, E. (2011). Ejector design and theoretical study of R134a ejector refrigeration cycle. International Journal of Refrigeration, 34(7), 1684-1698.

[20] Rogdakis, E. D., & Alexis, G. K. (2000). Investigation of ejector design at optimum operating condition. Energy Conversion and Management, 41(17), 1841-1849.

[21] Sokolov, M., & Hershgal, D. (1990). Enhanced ejector refrigeration cycles powered by low grade heat. Part 2. Design procedures. International Journal of Refrigeration, 13(6), 357-363.

[22] Abdel-Aal, H. K., Al-Zakri, A. S., El-Sarha, M. E., El-Swify, M. E., & Assassa, G. M. (1990). Other options of mass and energy input for steam jet refrigeration systems. The Chemical Engineering Journal, 45(2), 99-110.

[23] Selvaraju, A., & Mani, A. (2004). Analysis of an ejector with environment friendly refrigerants. Applied Thermal Engineering, 24(5-6), 827-838.

[24] Chen, J., Havtun, H., & Palm, B. (2014). Parametric analysis of ejector working characteristics in the refrigeration system. Applied Thermal Engineering, 69(1-2), 130-142.

[25] Sadeghi, M., Mahmoudi, S. M. S., & Saray, R. K. (2015). Exergoeconomic analysis and multi-objective optimization of an ejector refrigeration cycle powered by an internal combustion (HCCI) engine. Energy Conversion and Management, 96, 403-417.

[26] He, S., Li, Y., & Wang, R. Z. (2009). Progress of mathematical modeling on ejectors. Renewable and Sustainable Energy Reviews, 13(8), 1760-1780.

[27] Ouzzane, M., & Aidoun, Z. (2003). Model development and numerical procedure for detailed ejector analysis and design. Applied Thermal Engineering, 23(18), 2337-2351.

[28] Liu, F., & Groll, E. A. (2008). Analysis of a two phase flow ejector for transcritical co_2 cycle. In Proceedings of the International Refrigeration and Air Conditioning Conference, 924-930.

[29] Zucker, R., & Biblarz, O. (2002). Fundamentals of Gas Dynamic, 2nd ed.; John Wiley and Sons, INC: New York.

[30] Cengel, Y. A., Boles, M. A. (2001). Thermodynamics: An engineering approach. McGraw-Hill: Boston.

[31] Henry, R. E., & Fauske, H. K. (1971). The two-phase critical flow of one-component mixtures in nozzles, orifices, and short tubes. Journal of Heat Transfer, 93(2), 179-187.

[32] Chaiwongsa, P., & Wongwises, S. (2008). Experimental study on R-134a refrigeration system using a two-phase ejector as an expansion device. Applied Thermal Engineering, 28(5-6), 467-477.

[33] Hassanain, M., Elgendy, E., & Fatouh, M. (2015). Ejector expansion refrigeration system: Ejector design and performance evaluation. International Journal of Refrigeration, 58, 1-13.

[34] Tangren, R. F., Dodge, C. H., & Seifert, H. S. (1949). Compressibility effects in two-phase flow. Journal of Applied Physics, 20(7), 637-645.

[35] Banasiak, K., Hafner, A., & Palacz, M. (2015). State of the art in the identification of two-phase transonic flow phenomena in transcritical CO_2 ejectors, In Proceedings of the 24th IIR International Congress of Refrigeration, 80-88.

[36] Elbel, S. W., &Lawrence, N. (2016). Review of recent developments in advanced ejector technology. International Journal of Refrigeration, 62, 1-18.